Consequent-Pole Permanent-Magnet Machine With Extended Field-Weakening Capability

Juan A. Tapia, *Member, IEEE*, Franco Leonardi, *Member, IEEE*, and Thomas A. Lipo, *Fellow, IEEE*

***Abstract*—In this paper a description and operating principles of a consequent-pole permanent-magnet machine are presented. In addition, a sizing analysis, finite-element analysis, and experimental results for a prototype machine are addressed. Due to its particular configuration, this machine allows for a wide range of control of the air-gap flux with minimum field ampere-turn requirements and without brushes or slip rings. Two components of the field flux are produced. One, which is almost constant, is produced by the permanent magnet located on the rotor surface. The other, which is variable, is produced by a field winding positioned circumferentially in the center of the stator. These two flux components converge in the air gap. The excitation level of the machine is manipulated by controlling the dc field current. Three-dimensional finite-element analysis and experimental results demonstrate that it is possible to vary the flux over a wide range to keep the terminal voltage constant as the speed increases. A 3-kW 1000-3000-r/min eight-pole and 32-Vac generator using this configuration is tested to verify the flux control capability of this structure.**

***Index Terms*—Electric machine design, flux weakening, permanent-magnet (PM) machine.**

I. Introduction

DURING the last several decades permanent-magnet (PM) machine drives have increased in popularity in a wide variety of industrial applications for a number of reasons. Included in these reasons are higher power density and efficiency, higher reliability, and lower inertia. Moreover, the continuous reduction price of the PM material has reduced the material cost, and allows one to obtain reasonable prices for ac drives based on the PM machine. However, fixed excitation provided by the PM limits controllability of the drive and the high speed capability. Control of the excitation is essential in most alternator applications where cost consideration prevents the use of synchronous rectification. In ac drive applications, to extend the speed range, the machines are operated, such that the armature currents partially demagnetize the magnets achieving the so-called field weakening [1]–[3]. However, this approach involves the risk of irreversible demagnetization of the PMs and generates significant heat due to the I^2R losses. If the temperature and reverse d-axis flux are sufficiently high to move the operating point near or below the knee of the normal demagnetization point, irreversible changes in the PM properties occur.

To avoid this undesirable effect, alternative solutions have been reported. Nipp, in [4], suggests connecting groups of the stator winding in different configurations so that the induced voltage is adjusted accordingly. In [5], a stator-mounted PM machine is presented where the weakening process is obtained by changing the reluctance path of the magnet. Using a field winding to add or subtract flux from the PM is explained in [6]. In this case, magnet and winding control are located in the stator. In [7] a synchronous PM motor with two-section rotor with field weakening is analyzed. Here, the reluctance of the d-axis flux path is varied, changing the ratio between each section.

The purpose of this paper is to explore a magnetic structure termed the consequent-pole PM (CPPM) machine which has inherent field weakening capability. This machine combines the fixed excitation of the rare earth permanent magnet with the variable flux given by a field winding located on the stator. In this manner, air-gap flux can be controlled over a wide range with a minimum of conduction losses and without demagnetization risk for the PM pieces. For a 3-kW prototype using this configuration finite-element analysis (FEA) establishes that a modest amount of field Ampere-Turns (ATs) (less than 500 ATs) are necessary to vary the air-gap flux in a wide range ($\pm$40% of the no-DC field component). An ac generator has been built based on this concept. In Sections II–V, a description and operating principles are explained and design equation are derived.

II. Description and Operation of the CPPM Machine

A. Description

Fig. 1 shows the structure of the CPPM machine. The machine consists of a rotor divided into two sections. One section has partial surface-mounted PMs, which are radially magnetized, and the other has a laminated iron pole. A yoke of solid iron connects these two sections. The stator is composed of a laminated core, solid iron yoke, and a conventional ac three-phase winding allocated in slots around the periphery of the inner diameter. To complete the stator structure, a circumferential field winding is placed in the middle of the stator, which is excited by a dc current. The solid stator and rotor yoke provide a low reluctance path for the axial flux, which is an important component in the machine's operation. The current of the field winding is externally controlled to provide variable excitation.

Paper IPCSD 03–074, presented at the 2001 IEEE International Electric Machines and Drives Conference, Cambridge, MA, June 17–20, and approved for publication in the IEEE TRANSACTIONS ON INDUSTRY APPLICATIONS by the Electric Machines Committee of the IEEE Industry Applications Society. Manuscript submitted for review April 25, 2002 and released for publication July 22, 2003. This work was supported by the Wisconsin Electrical Machines and Power Electronics Consortium (WEMPEC), and by the Fondo de Desarrollo Cientifico y Tecnologico-Chile (FONDECYT Project 1030329).

J. A. Tapia is with the Department of Electrical Engineering, University of Concepción, Concepción, Chile (e-mail: Jtapia@die.udec.cl).

F. Leonardi is with the Vehicle Electronic Systems Department, Ford Research Laboratories, Dearborn, MI 48120 USA (e-mail: leonar2@ford.com).

T. A. Lipo is with the Department of Electrical and Computer Engineering, University of Wisconsin, Madison, WI 53706-1651 USA (e-mail: lipo@engr.wisc.edu).

Digital Object Identifier 10.1109/TIA.2003.818993

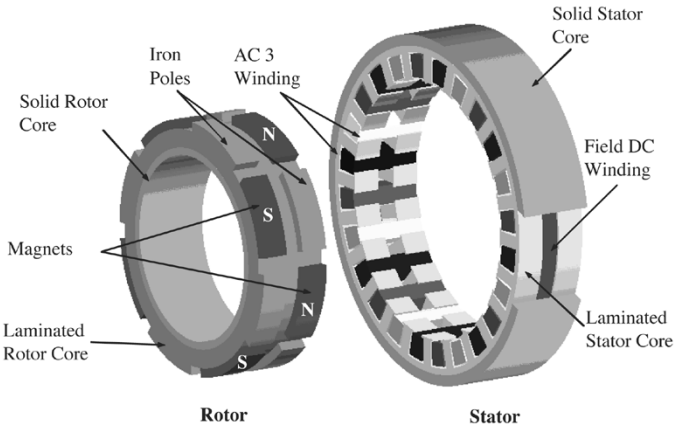

Fig. 1. Magnetic structure of the CPPM machine.

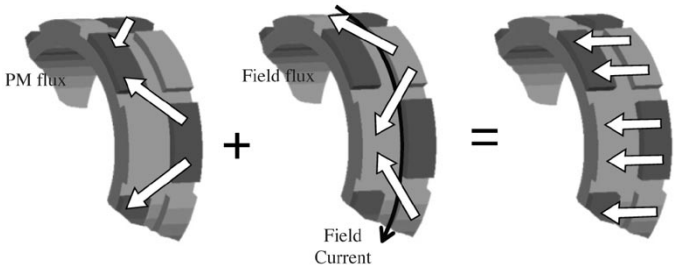

Fig. 2. Demagnetizing effect of the field flux.

B. Operation

The radial magnetization of the PMs creates a nearly constant flux, which circulates from one pole to the next across the stator and rotor yoke, teeth and PM pieces. This portion of the flux is determined mainly by the geometry of the PM and the reluctance of its path. In this case, the air-gap and magnet reluctances are the most important values. On the other hand, injecting dc current into the field winding, generates a flux which flows from one iron pole to the next pole through the stator and rotor yoke, with a path entirely composed by iron, except for the main air gap. Due to the comparatively low reluctance of this path, the DC current flowing in the field winding is reduced and this flux component can be easily controlled. The two fluxes combine in the air gap, and the effect of the winding generated flux goes to add or subtract to pm flux according to the field current polarity.

1) Demagnetizing Effect of the DC Field Winding: If the flux generated by the dc current circulating into the field winding flows in such direction that it is subtracted to the flux of the PM the flux per pole closes its path in the same magnetic pole. Fig. 2 depicts this operating condition. In fact, in the air gap, flux emanating from the PM and the iron pole are cross the air gap in opposite directions. As a result, the total flux per pole decreases as the field current increases. Flux essentially crosses the stator yoke axially.

2) Magnetizing Effect of the DC Field Winding: If the dc field current is reversed, the field flux uses the magnetic circuit as before, but flows in the opposite direction. Therefore, both components of the air-gap flux cross the air gap in the same direction. Consequently, as the dc field current increases, the flux per pole increases. Flux closes its path crossing the stator yoke essentially tangentially as is shown in Fig. 3.

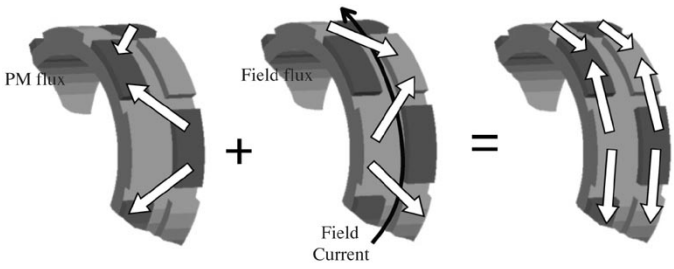

Fig. 3. Magnetizing effect of the field flux.

C. Features

The CPPM machine presents several advantages in comparison with the conventional PM machine such as the following.

- A wide range of air-gap flux control is obtained with a low field AT requirement. This control can be used to either reduce or increase the air-gap flux.
- The CPPM machine magnetic configuration allows one to control the air-gap flux level without any demagnetization risk for the magnet pieces. Control action is performed over low-reluctance iron poles.
- A simple dc current control is used and no brushes or slip rings are required to perform this control. Field control winding is allocated in a special slot in the stator.

D. Drawbacks

However, the CPPM machine presents some drawback due to its configuration.

- Additional dc winding in the stator reduces the power density. The required space reduces inner diameter and/or increases the outer diameter. In addition, air-gap surface associated to this winding does not participate in the energy conversion process.
- Three-dimensional (3-D) flux distribution introduces extra losses and increases material requirement. Stator and rotor core require tangential and axial flux conduction capacity. Additionally, there are some manufacturing problems.

III. Electromagnetic Design

In order to obtain adequate dimensions for the prototype to be built a set of equations are derived to relate mechanical dimensions, electromagnetic restrictions, and technical constraints. Finally, an optimization based on surface current density and minimum total volume of the machine is carried out to obtain optimum geometry.

A. Air-Gap Flux

By dividing the air-gap surface in two sections, one corresponding to the permanent magnet and the other one to the iron pole areas, the total air-gap flux can be divided into two components associated with each of these sections: $\phi_{g-\mathrm{iron}}$ and $\phi_{g-\mathrm{pm}}$ (see Fig. 4). If excitation current of the field winding is injected, with a positive or negative polarity, flux of the iron pole section will change linearly if the iron saturation is neglected. On the other hand, flux associated with the permanent magnet will be invariant. Superposition of these two fluxes results in the total

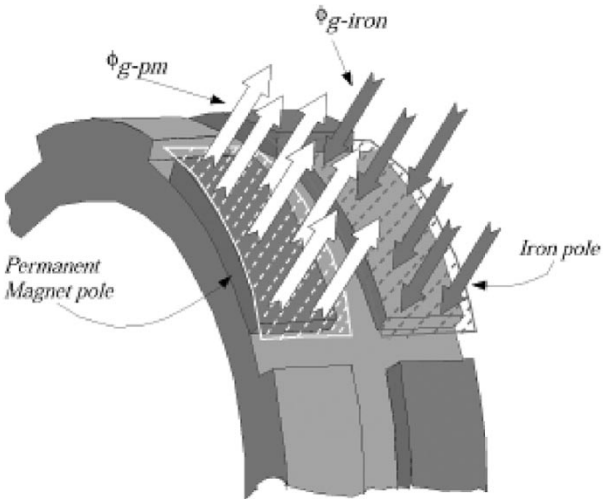

Fig. 4. Air-gap flux components.

air-gap flux. This resultant flux can be either the summation or subtraction of each component. Therefore, the air-gap flux can be expressed as

$$\phi_g = \phi_{g-\mathrm{iron}} + \phi_{g-\mathrm{pm}} \tag{1}$$

where

$$\phi_{g-\mathrm{iron}} = \mu_o \frac{N_{fl} I_{fl}}{2 g_e A_g} \tag{2}$$

where $N_{fl}I_{fl}$ are the field ATs, g_e is the equivalent air-gap length affected by Carter's coefficient, and A_g is the air-gap area. The field current I_{fl} is positive for magnetizing flux, negative for demagnetizing.

The second term of (1) is

$$\phi_{g-\mathrm{pm}} = \frac{2R_{\mathrm{pm}} \parallel R_{lg}}{2R_g + 2R_{\mathrm{pm}} \parallel R_{lg}} \Phi_r \tag{3}$$

where R_{pm}, R_{lg}, and R_g are the PM, leakage, and air-gap reluctance, respectively, and ϕ_r is the remanent flux due to the PM remanence.

Equations (2) and (3) show the decoupled effect between each air-gap flux components. The $\phi_{g-\mathrm{iron}}$ is primarily dependent on the dc current: its magnitude and direction. Conversely, the $\phi_{g-\mathrm{pm}}$ is mainly a function of the PM magnetic parameters. Under no saturation, both components cross the air gap by independent path: iron and PM poles. As a result, low field AT is required to the manipulate iron flux component, and there is no demagnetizing action over the magnet.

B. Stator Tooth Dimensions

Analyzing the actual flux distribution in Section III-A, it is found that due to the necessary space required to allocate the field winding, the most critical condition for the stator yoke flux is when fluxes are crossing the air gap in opposite directions, flowing from the PM to the iron pole (see Fig. 5). In effect, the total area to circulate the flux for this operating condition is reduced to that defined by d_c (Fig. 6).

Following a similar procedure as is given by Honsinger and Lipo in [8] and [9], equations are obtained considering this extreme operating condition. Based on maximum values of flux

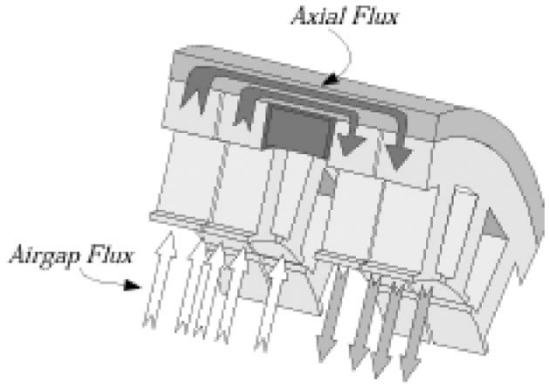

Fig. 5. Flux path in the stator yoke for the demagnetizing condition.

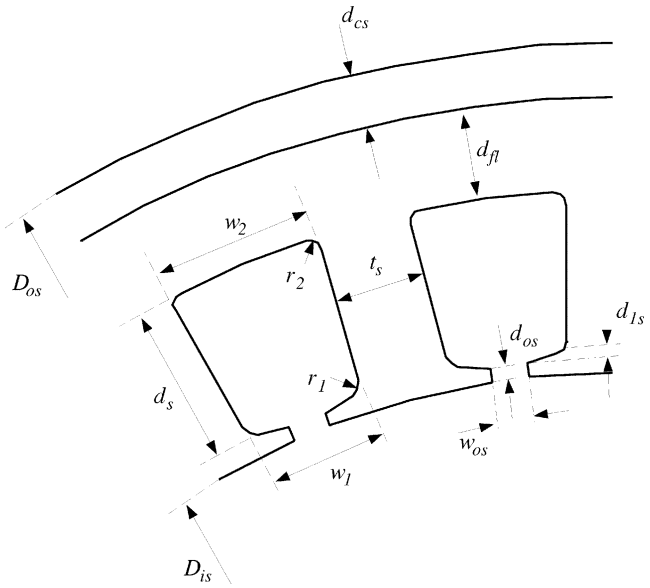

Fig. 6. Stator slot dimensions.

density in the air gap B_g, stator tooth B_t, and yoke B_c, expressions for tooth width and axial stator yoke thickness are given by (4) and (5)

$$t_s = \frac{B_g}{B_t} \frac{D_{is}}{K_s K_{lg} S_1} \pi. \tag{4}$$

Under the same argument, the flux crossing either iron pole or PM section crosses the stator yoke axially. Considering similar flux density in both sections, the yoke depth is calculated by

$$d_{cs} = \frac{B_g}{K_{lg} B_c} D_{is} K_a. \tag{5}$$

K_a is defined as

$$K_a = \frac{l_{\mathrm{pm}}}{D_{os}}. \tag{6}$$

This index is referred to as the "external aspect ratio" and represents the proportion between the axial length (active length) and the outer diameter of the machine. Notice that d_{cs} does not depend of the number of poles as it does for a radial machine. In fact, as the number of poles increases in a regular radial or axial flux machine, the amount of flux per pole is reduced if

the peak flux density is the same [9]. Therefore, the yoke thickness can be smaller, reducing the outer diameter. However, in the CPPM machine with a fixed outer diameter, as K_a increases the amount of flux per pole also increases (larger value of $l_{\rm pm}$). As a result, the stator yoke increases in thickness and the inner diameter must decrease to maintain a reasonable value of B_c.

C. AC Slot Area

According to Fig. 6, the following expression for the slot dimensions can be obtained:

$$w_1 = \frac{\pi}{S_1} D_{is} - G_t \frac{D_{is}}{K_s S_1} \pi \tag{7}$$

and

$$w_2 = \frac{\pi}{S_1} \left[D_{os} - 2(d_{fl} + G_c D_{is} K_a) \right] - t_s \tag{8}$$

where

$$G_t = \frac{B_g}{K_s K_{lg} B_t} \tag{9}$$

$$G_c = \frac{B_g}{K_s B_c}. \tag{10}$$

From the same figure,

$$D_{os} = D_{is} + 2(d_{cs} + d_{fl} + d_s) \tag{11}$$

and with (7), (8), and (11), the slot depth can be expressed as

$$d_s = \frac{S_1}{2\pi}(w_2 - w_1). \tag{12}$$

Using the same approximations for (7) and (8), the slot area is

$$A_{slot} = \frac{ds}{2}(w_2 + w_1) \tag{13}$$

and with (12), this expression becomes

$$A_{slot} = \frac{S_1}{4\pi}(w_2 - w_1)(w_2 + w_1). \tag{14}$$

Introducing (7) and (8) into the previous equation, the slot area can be expressed as

$$A_{slot} = \frac{\pi D_{os}^2}{4 S_1} \left[a \left(\frac{D_{is}}{D_{os}} \right)^2 - 2b \left(\frac{D_{is}}{D_{os}} \right) + 1 \right] \tag{15}$$

where $a = 2G_t + 2G_c G_t K_a + (G_c K_a)^2 - 1$ and $b = G_t + G_c K_a$.

The right side of (15) represents a quadratic equation with the inner–outer diameter ratio as a variable. There is an optimum value of this ratio which maximizes the slot area with G_c and G_t as parameters.

D. DC Field Slot Area

The area required to allocate the dc field winding is obtained as the product between the axial, l_{fl}, and the radial, d_{fl}, lengths

$$A_{fl} = d_{fl} l_{fl}. \tag{16}$$

Defining K_{fl} as the ratio between these two variables,

$$K_{fl} = \frac{l_{fl}}{d_{fl}} \tag{17}$$

and (16) can be rewritten as

$$d_{fl}^2 = \frac{A_{fl}}{K_{fl}}. \tag{18}$$

TABLE I
CPPM MACHINE PROTOTYPE DATA

Stator outer diameter	168	mm
Stator inner diameter	118	mm
Stack length	40	mm
Pole axial length	15	mm
poles	8	
phases	3	

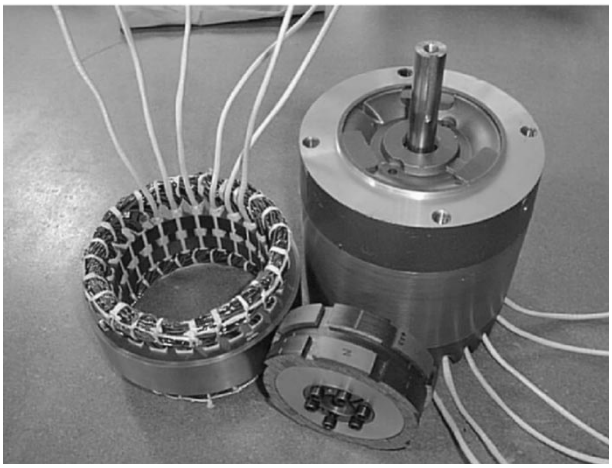

Fig. 7. Prototype.

On the other hand, this area is also defined by the number of conductors N_{fl} and copper area $A_{fl-\rm cond}$:

$$A_{fl} = N_{fl} \frac{A_{fl-\rm cond}}{K_{\rm cu}} \tag{19}$$

where K_{cu} is the fill factor. For a given application, the amount of mmf_{fl} required to reach a particular flux density condition is calculated from (2).

$$B_{g-\rm iron} = \left| \mu_o \frac{N_{fl} I_{fl}}{2g} \right|. \tag{20}$$

Solving (20) for N_{fl} and inserting this result in (19), the expression for the dc slot area becomes

$$A_{fl} = B_{g-\rm iron} \frac{2 g_e K_{\rm cu}}{\mu_o J_{fl}}. \tag{21}$$

This last equation establishes that the geometry of the dc field slot is defined primarily for the air-gap flux density of the iron portion, which is proportional to the field ATs, and the field current density.

E. Prototype

Based on the previous equation, an optimization process has been carried out and a 3-D FEA used to calculate the magnetomotive force (MMF) field required for a 3-kW eight-pole CPPM machine prototype. Main data of the prototype are shown in Table I. Fig. 7 shows the CPPM machine prototype.

IV. FEA

FEA was used to determine flux distribution and the field-weakening capability of the prototype. Fig. 8 shows the air-gap flux for three different conditions of the DC field current. From this result, it is possible to observe that the flux over the PM

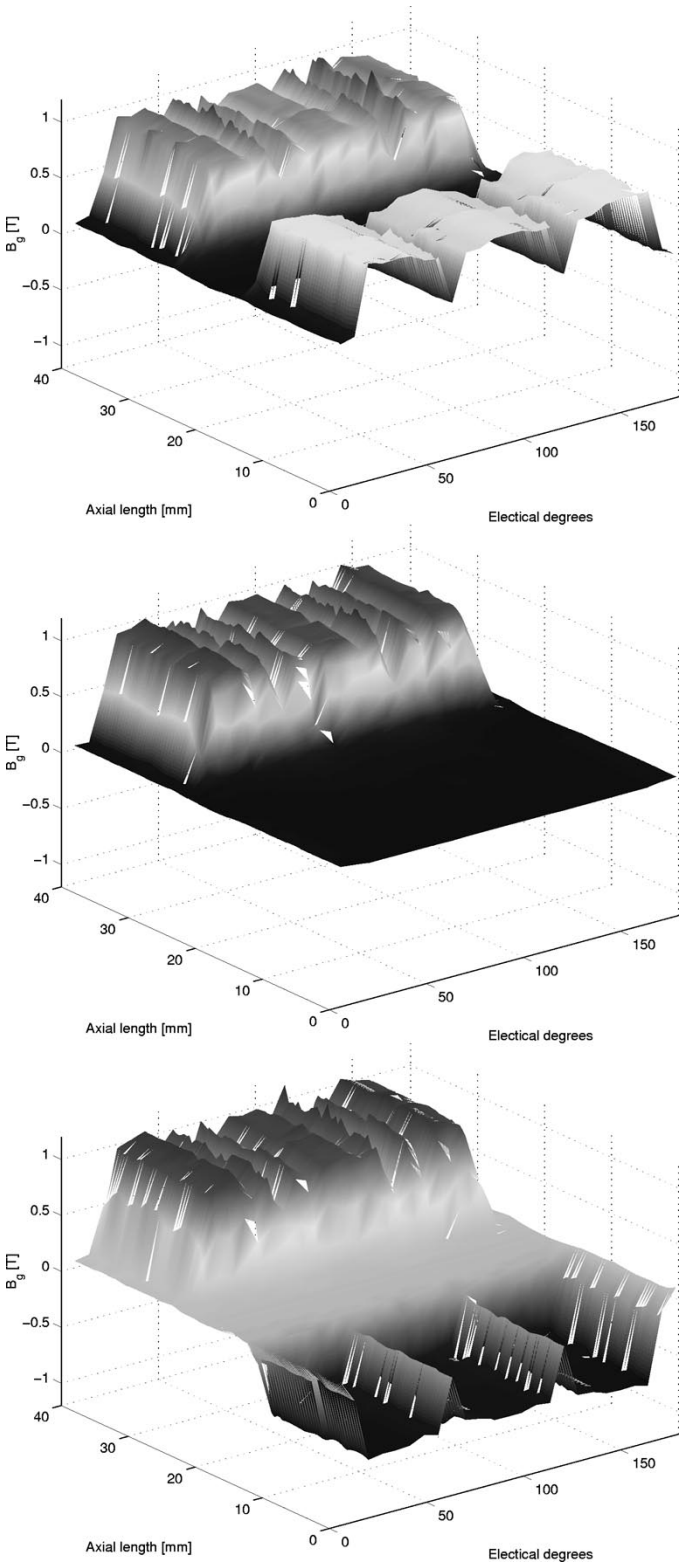

Fig. 8. Air-gap flux distribution for different field ATs. (a) 500 ATs with magnetizing effect. (b) No field current. (c) 500 ATs with demagnetizing effect.

is unidirectional with an almost constant magnitude. However, the direction of the flux over the iron pole surface changes according to the magnitude and polarity of the dc field current. It is clear that the action of the field flux is concentrated primarily over the iron pole, with no demagnetizing effect over the PM piece. These two components make the total air-gap flux vary,

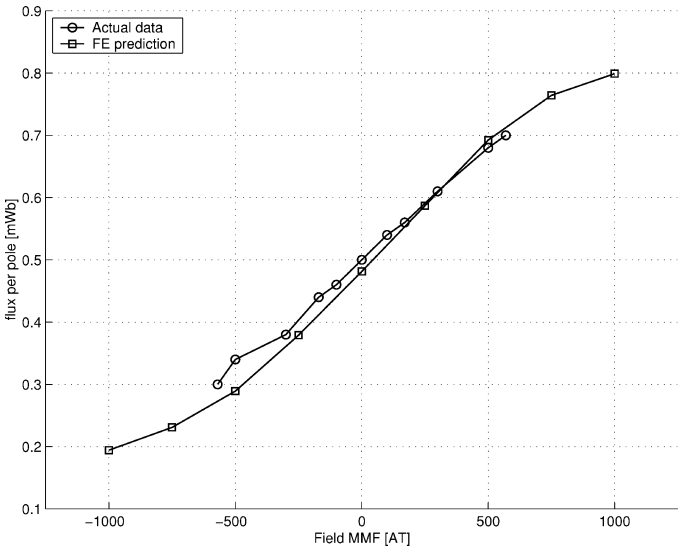

Fig. 9. FE analysis and experimental result.

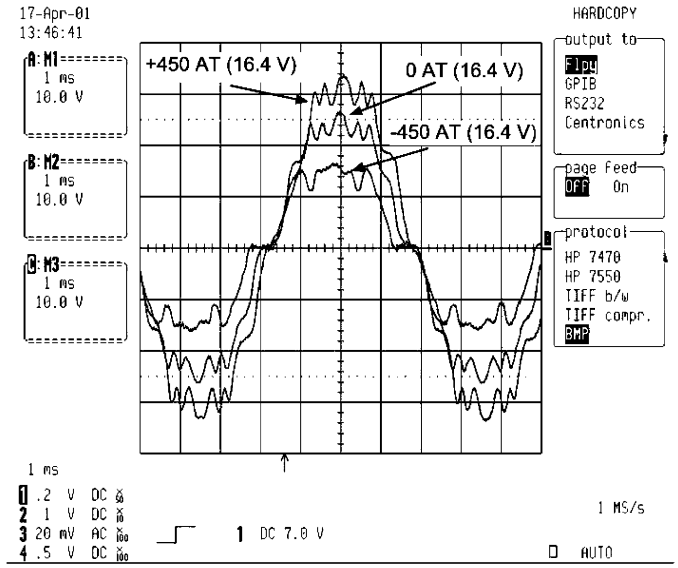

Fig. 10. Back EMF for different field ampere-turns.

either weakening or boosting the air-gap flux from the nonfield current condition. Numerically, FEA predicts that the air-gap flux changes with a variation $\pm 40\%$ with respect to the no-field excitation. This operation is depicted in Fig. 9.

V. Experimental Result

Experimental fluxes per pole obtained from the prototype are compared with calculated values from FEA in Fig. 9. Linear flux control is obtained for the field AT range tested. It can be seen that a wide range of flux control can be achieved with a modest amount of field MMF. With a variation of ± 500 ATs, the flux per pole vary in a range of 0.28–0.77 mWb, with 0.5 mWb under no-field excitation.

Fig. 10 shows the field control capability. The measured no-load output voltage is presented for a machine speed of 1500 r/min. Increases and decreases of the output voltage with respect to the zero dc field current condition are obtained.

VI. Conclusion

In this paper, the description and operating principles of the CPPM machine have been presented. Its magnetic structure allows for easy control of the air-gap flux over a wide range, using only a modest amount of field ATs. The required control is obtained by injecting a dc current in a stationary field winding located in the center portion of the stator. As a result, no sliding parts are necessary to perform such field control. Additionally, there is no risk of demagnetization for the magnet because the control action is exercised over the iron poles.

Stator and rotor core require special features to conduct flux in three dimensions. In fact, interlamination air gaps increase the reluctance degrading the dc field control range.

For analysis purposes, air-gap flux can be easily separated in two components proportional to field flux and PM magnetic characteristics. Expressions for the ac winding slot and dc field slot areas expression have been derived. The inner-outer diameter ratio and field ATs are the primarily variables which define each of these areas.

Experimental and FEA results agree that the field weakening/boosting can be achieved with a modest requirement for field current.

References

[1] Y. Sozer and D. A. Torrey, "Adaptive flux weakening control of permanent magnet synchronous motor," in *Conf. Rec. IEEE-IAS Annu. Meeting*, vol. 1, St. Louis, MO, 1998, pp. 475–482.

[2] W. L. Soong and T. J. Miller, "Field-weakening performance of brushless synchronous AC motor drives," *Proc. IEE—Elect. Power Applicat.*, vol. 141, no. 6, pp. 331–340, Nov. 1994.

[3] S. R. Macminn and T. M. Jahns, "Control techniques for improved high-speed performance of interior PM synchronous motor drives," *IEEE Trans. Ind. Applicat.*, vol. 27, pp. 997–1004, Sept./Oct. 1991.

[4] E. Nipp, "Alternative to field-weakening of surface-mounted permanent-magnet motors for variables-speed drives," in *Conf. Rec. IEEE-IAS Annu. Meeting*, vol. 1, 1995, pp. 191–198.

[5] A. Shakal, Y. Liao, and T. A. Lipo, "A permanent magnet AC machine structure with true fied weakening capability," in *Conf. Rec. IEEE Int. Symp. Industrial Electronics*, 1993, pp. 19–24.

[6] F. Leonardi, P. J. McCleer, and T. Lipo, "The DSPM: An AC permament magnet traction motor with true field weakening," presented at the 2nd Int. Conf. All Electric Combat Vehicle, Detroit, MI, June 1997.

[7] B. J. Chalmers, R. Akmese, and L. Musaba, "Design and field-weakening perfomance of permanent-magnet/reluctance motor with two-part rotor," *Proc. IEE—Elect. Power Applicat.*, vol. 145, no. 2, pp. 133–139, Mar. 1998.

[8] V. B. Honsinger, "Sizing equations for electrical machinery," *IEEE Trans. Energy Conversion*, vol. EC-2, pp. 116–121, Mar. 1987.

[9] T. A. Lipo, "Electromechanical machine design," in *Classroom Text for ECE 713*. Madison, WI: Univ. of Wisconsin, 1995.

Juan A. Tapia (M'03) was born in Concepción, Chile. He received the B.E.E. and M.E.E degrees in electrical engineering from the University of Concepción, Concepción, Chile, in 1991 and 1997, respectively, and the Ph.D. degree from the University of Wisconsin, Madison, in 2002.

Since 1992, he has been with the Department of Electrical Engineering, University of Concepción, as an Assistant Professor. His primary areas of interest are electromechanical analysis and electrical machines design for ac adjustable-speed applications.

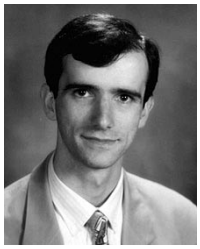

Franco Leonardi (S'93–M'96) received the Degree and the Doctorate degree in electrical engineering from the Universita degli Studi di Padova, Padova, Italy, in 1991 and 1995, respectively.

From 1994 to 1996, he was at the University of Wisconsin, Madison, where he worked on synchronous reluctance and doubly salient permanent-magnet motors. In 1996, he joined McCleer Power, Inc., Jackson, MI, where he worked on traction applications of electric machines and other R&D projects for passenger and off-road vehicles and where, in 1998, he was appointed Vice President of Engineering. Since 1999, he has been with the Vehicle Electronic Systems Department, Ford Research Laboratories, Ford Motor Company, Dearborn, MI, where he is involved in the development of hybrid electric vehicles and the 42-V PowerNet.

Thomas A. Lipo (M'64-SM'71-F'87) was born in Milwaukee, WI. He received the B.E.E. and M.S.E.E. degrees from Marquette University, Milwaukee, WI, in 1962 and 1964, respectively, and the Ph.D. degree in electrical engineering from the University of Wisconsin, Madison, in 1968.

From 1969 to 1979, he was an Electrical Engineer in the Power Electronics Laboratory of Cooperate Research and Development of the General Electric Company, Schenectady, NY. He became a Professor of Electrical Engineering at Purdue University, West Lafayette, IN, in 1979, and in 1981, he joined the University of Wisconsin, Madison, in the same capacity, where he is presently the W. W. Grainger Professor for Power Electronics and Electrical Machines, Co-Director of the Wisconsin Electric Machines and Power Electronics Consortium, and Director of the Wisconsin Power Electronics Research Center. He has authored 400+ published technical papers and is the holder of 32 U.S. patents.

Dr. Lipo has received the 1986 Outstanding Achievement Award from the IEEE Industry Applications Society (IAS), William E. Newell Award of the IEEE Power Electronics Society, and the 1995 Nicola Tesla IEEE Field Award from the IEEE Power Engineering Society for his work. He has served the IEEE in various capacities for three IEEE Societies, including President of the IAS. He is a Fellow of the Institution of Electrical Engineers, U.K., and the Royal Academy of Engineering (Great Britain), and a Member of the Institute of Electrical Engineers of Japan. He has received 21 IEEE Prize Paper Awards from three different IEEE Societies including Best Paper Awards for publication in the IEEE Transactions in the years 1984, 1994, and 1999.